2011

Suppression of GSK-3 activation by M-cadherin protects myoblasts against mitochondria-associated apoptosis during myogenic differentiation

Y. Wang

Y. Hao

S. E. Alway

Suppression of GSK-3β activation by M-cadherin protects myoblasts against mitochondria-associated apoptosis during myogenic differentiation

Yan Wang, Yanlei Hao* and Stephen E. Alway‡

Laboratory of Muscle Biology and Sarcopenia, Division of Exercise Physiology, and Center for Cardiovascular and Respiratory Sciences, Robert C. Byrd Health Sciences Center, West Virginia University School of Medicine, Morgantown, West Virginia 26506, USA

*Present address: Department of Neurology, Affiliated Hospital of Jining Medical College, Jining, China

‡Author for correspondence (salway@hsc.wvu.edu)

Accepted 23 June 2011
Journal of Cell Science 124, 3835–3847

doi: 10.1242/jcs.086686

Summary

Apoptosis occurs concurrently with differentiation of muscle progenitor cells (MPCs) before they fuse to form myotubes. Dysregulated apoptosis in MPCs contributes to the low regeneration capability in aged muscle and decreases the survival rate of donor cells in stem cell-based therapies for muscular dystrophies. This study investigated the role of the M-cadherin/PI3K/Akt/GSK-3β signaling pathway in regulating apoptosis during differentiation of MPCs. Disruption of M-cadherin-dependent cell–cell adhesion by M-cadherin RNA interference in confluent C2C12 myoblasts sensitized the cells to mitochondria-associated intrinsic apoptosis induced by cell confluence or serum starvation. Further investigation of this pathway revealed that M-cadherin-mediated signaling suppressed GSK-3β activation by enhancing the PI3K/AKT-dependent inhibitory phosphorylation of Ser9 in GSK-3β. Overexpression of wild-type GSK-3β in confluent C2C12 myoblasts exacerbated the apoptosis, whereas chemical inhibition of GSK-3β using TDZD-8, or forced expression of constitutively active Akt (myrAkt), or a kinase-deficient GSK-3β mutant [GSK-3β(K85R)], attenuated apoptosis and rescued the impaired myogenic differentiation that is caused by M-cadherin RNA interference. These data suggest that M-cadherin-mediated signaling prevents acceleration of mitochondria-associated intrinsic apoptosis in MPCs by suppressing GSK-3β activation during myogenic differentiation.

Key words: M-cadherin, Myoblasts, Apoptosis, Myogenesis

Introduction

Muscle progenitor cells (MPCs) or satellite cells remain quiescent both metabolically and mitotically in adult muscles under normal basal physiological conditions. Once activated by stimuli such as muscle injury or exercise, they enter the cell cycle, proliferate, differentiate and fuse into myotubes for muscle regeneration (Seale and Rudnicki, 2000; Zammit et al., 2006). The differentiation of MPCs is critical for myotube formation, but it also occurs concurrently with apoptosis (Dee et al., 2002; Walsh, 1997). Apoptosis is a systematic process of programmed cell death that is important for normal tissue morphogenesis and development by maintaining the tissue homeostasis. The dysregulation of apoptosis contributes to a variety of pathologies, including cancer, autoimmune diseases, cardiovascular disease and degenerative neurological diseases (Baehrecke, 2002; Quadrilatero and Bloemberg, 2010; Quadrilatero and Rush, 2008). In skeletal muscle, apoptosis has been linked to conditions of muscle wasting caused by disuse, denervation and aging (Alway and Siu, 2008; Siu et al., 2005a; Siu et al., 2005c). In addition, inappropriate apoptosis of muscle progenitor cells might contribute to the low regeneration capability of dystrophic muscles and the poor outcomes of stem-cell-based therapeutic strategies (Gussoni et al., 1997; Partridge et al., 1998; Tews and Goebel, 1997; Tidball et al., 1995). Decreased muscle progenitor cell number (Day et al., 2010), function (Corbu et al., 2010; Leiter and Anderson, 2010) and altered responses to their niche (Brack and Rando, 2007; Conboy et al., 2005) contribute to the impaired regenerative capability in aging skeletal muscle. In addition, muscle progenitor cells that are isolated from aged muscle are susceptible to apoptosis, and their number declines because more of them are depleted by apoptosis in aged muscle (Collins et al., 2007; Jejurikar et al., 2006; Jejurikar and Kuzon, 2003).

M-cadherin is a member of the classical cadherin family of transmembrane glycoproteins mediating calcium-dependent homophilic cell–cell adhesion. M-cadherin is specifically expressed in skeletal muscle and certain neural tissues. In mature skeletal muscle, M-cadherin is only detectable on satellite cells and the underlying sarcolemma of myofibers (Irintchev et al., 1994; Kaupmann et al., 1992). The number of M-cadherin-positive satellite cells decreases in aged muscle (Sajko et al., 2004). Although a mouse knockout model indicated that M-cadherin might play a dispensable role in myogenesis and muscle regeneration in vivo (Hollnagel et al., 2002), data from in vitro studies showed that by interacting with Rac1 and other members of Rho subfamily, M-cadherin is critical in mediating myoblast alignment and fusion into myotubes (Charrasse et al., 2006; Charrasse et al., 2007; Wrobel et al., 2007). However, its role in regulating the survival and death of muscle progenitor cells or myoblasts has never been addressed.

In the present study, we investigated the role of M-cadherin-dependent cell–cell adhesion on the survival of mouse C2C12 myoblasts as well as primary muscle progenitor cells during

myogenic differentiation. We were particularly interested in the potential for M-cadherin to protect against the mitochondria-associated intrinsic apoptosis that is induced by cell confluence or serum starvation. By disrupting M-cadherin-dependent cell–cell adhesion by knocking down M-cadherin expression using RNA interference, we demonstrated that M-cadherin-mediated signaling is important for maintaining mitochondrial integrity. This occurred by suppressing GSK-3β activation in a

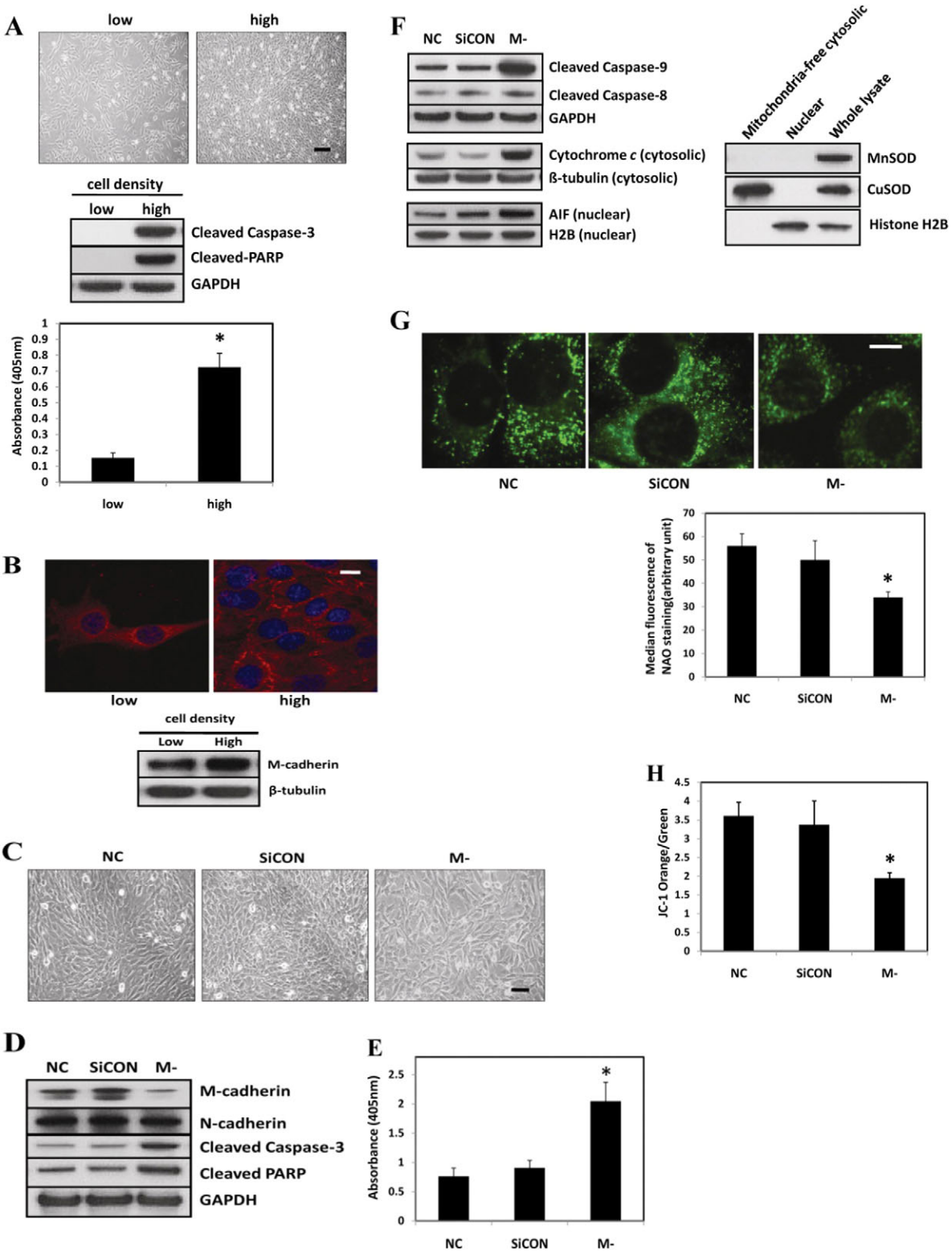

Fig. 1. See next page for legend.

PI3K/Akt-dependent manner, and reducing apoptotic signaling through the mitochondrial pathway, thus promoting the survival of myoblasts during myogenic differentiation. Moreover, apoptosis and impaired myogenic differentiation that is caused by reducing M-cadherin protein abundance could be rescued by the inhibition of GSK-3β activation. Together, these results suggest an indispensable role of M-cadherin-mediated signaling in maintaining the balance between apoptosis and differentiation of muscle progenitor cells during myogenesis and potentially during activation of muscle stem cells such as that occurring during muscle regeneration.

Results

M-cadherin RNA interference exacerbates mitochondria-associated apoptosis in confluent C2C12 myoblasts

To evaluate the apoptotic propensity to high and low cell densities, C2C12 myoblasts were seeded in six-well plates at either $2.0\times10^3/cm^2$ to obtain a low density (~20–30% confluent) or $2.1\times10^4/cm^2$ to reach a high cell density (~100% confluent) within 48 hours. The phase-contrast images in the top panel of Fig. 1A show typical morphology of C2C12 myoblasts at low or high cell densities. The protein abundance of cleaved caspase-3 and Poly (ADP-ribose) polymerase (PARP) was markedly increased in fully confluent cells when compared with cells that were plated at a low density (Fig. 1, middle panel). The cleavage of PARP by caspases leads to nuclear DNA fragmentation. Furthermore, a cell-death ELISA assay showed an elevation of cytosolic nucleosomes at full cell confluence (Fig. 1A, bottom panel). This provided additional evidence for an increase in apoptotic DNA fragmentation in confluent cells compared with non-confluent cells. We next explored the expression pattern and level of M-cadherin at different cell densities. M-cadherin was located diffusely throughout the cells that were plated at a low density (Fig. 1B, top left panel). By contrast, M-cadherin relocated to cell–cell contacts at the periphery of the cells when they were confluent (Fig. 1B, top right panel). The protein abundance of M-cadherin increased in confluent C2C12 myoblasts compared with the non-confluent cells (Fig. 1B, bottom panel). To investigate the role of M-cadherin in regulating myoblast survival and apoptosis, we inhibited M-cadherin expression in confluent C2C12 myoblasts by transient transfection with M-cadherin-targeted small interfering RNA. Knockdown of M-cadherin expression in confluent C2C12 myoblasts caused a disruption in the cell–cell contacts and this increased the separation between the cells (Fig. 1C). Cells in the control group adhered tightly to each other as the cells became confluent (Fig. 1C). The knockdown of M-cadherin was verified by immunoblotting (Fig. 1D). The protein abundance of N-cadherin in C2C12 cells was not affected by M-cadherin RNAi treatment (Fig. 1D). However, M-cadherin RNAi exacerbated cell-confluence-induced apoptosis in C2C12 cells as determined by the increased protein abundance of cleaved caspase-3 and cleaved PARP (Fig. 1D). An increase in DNA fragmentation as measured by a cell death ELISA assay (Fig. 1E) confirmed that M-cadherin RNAi increased the level of cell-confluence-induced apoptosis.

Apoptosis is initiated in muscle by three pathways. These include the extrinsic death-receptor-mediated pathway, the intrinsic mitochondrial-dysfunction-associated pathway and the intrinsic ER-dysfunction-associated pathway (Adams, 2003; Alway et al., 2011; Alway and Siu, 2008). To determine which apoptotic pathway is involved in cell death caused by M-cadherin RNAi, we examined the activation status of caspase-9 and caspase-8, which are representative initiation caspases for the intrinsic or the extrinsic apoptotic pathway, respectively. The protein abundance of cleaved caspase-9, but not caspase-8, was markedly increased in response to M-cadherin RNAi (Fig. 1F). In addition, the protein abundance of cytosolic cytochrome *c* and nuclear apoptosis inducing factor (AIF) were also increased upon M-cadherin RNAi. This suggests that the apoptosis induced by M-cadherin RNAi is mediated by the intrinsic mitochondria-associated pathway. To further investigate the impact of M-cadherin RNAi on mitochondria as a mediator of apoptosis, we examined the cardiolipin content of the inner mitochondrial membrane of live cells using Nonyl Acridine Orange (NAO) staining. NAO is a metachromatic dye that binds specifically to the mitochondrial cardiolipin and its fluorescence intensity is an indicator of mitochondrial integrity (Jahnke et al., 2009; Ott et al., 2007). The median fluorescence intensity of NAO staining in cells treated with siRNA to knock down M-cadherin was significantly lower than that in control cells (Fig. 1G). This indicates that the integrity of mitochondria in C2C12 cells was disrupted after M-cadherin RNAi. Furthermore, the mitochondria membrane potential ($\Delta\psi_{mt}$) was also disrupted by reducing M-cadherin in confluent cells, as shown by a decrease in the orange and the increase in the green signals from treated mitochondria compared with control mitochondria after incubation with the fluorescent probe JC-1 (Fig. 1H). JC-1 is a mitochondria-permeable lipophilic cation that changes its color from orange to green as the $\Delta\psi_{mt}$ decreases. A reduced $\Delta\psi_{mt}$ results in shifts

Fig. 1. Effect of M-cadherin RNAi on apoptosis in confluent C2C12 myoblasts. (**A**) Representative phase-contrast images of C2C12 myoblasts obtained 48 hours after seeding at low density ($2.0\times10^3/cm^2$) or high density ($2.1\times10^4/cm^2$) (top). Scale bar: 200 μm. Immunoblots of cleaved caspase-3 and PARP obtained 48 hours after plating (middle). Cytosolic nucleosomes of low- or high-density cells were measured as an indication of apoptotic DNA fragmentation (bottom). Each data point represents the mean ± s.e.m. of three independent experiments. *$P<0.05$ vs the low-density group. (**B**) Expression pattern and protein abundance of M-cadherin at low and high cell densities. Representative confocal images of M-cadherin (red) and DAPI (blue) staining in C2C12 myoblasts at low or high cell density as described in A (top). Scale bar: 10 μm. Immunoblotting analysis of protein abundance of M-cadherin. β-tubulin was probed as a loading control (bottom). (**C–H**) 80% confluent C2C12 myoblasts were transfected with M-cadherin-targeted siRNA (M-) or non-targeted scramble siRNA (SiCON) as a control. Non-transfected cells with identical culture conditions were used as a normal control (NC) cells. The cells were harvested 48 hours after transfection. Each data point is the mean ± s.e.m. of three independent experiments. *$P<0.05$ vs the control groups. (C) Phase-contrast images of transfected cells. Scale bar: 100 μm. (D) Immunoblot analysis of transfected cells. (E) The apoptotic DNA fragmentation of transfected cells is shown as mean ± s.e.m. of three independent experiments. *$P<0.05$ vs both NC and SiCON control groups. (F) Proteins associated with apoptotic signaling (and the relevant control proteins) measured in transfected and control cells (left). The integrity and purity of protein subcellular fractions was verified by immunoblotting with appropriate control antibodies (right). (G) Digital images from control or transfected C2C12 cells stained with NAO (top). Scale bar: 20 μm. The median fluorescence intensity of NAO per cell was determined (bottom). The data are mean ± s.e.m. of three experiments. (H) Mitochondria were isolated from control and transfected cells and stained with JC-1. The data represent FACS analyses of the ratio of orange (intact mitochondria) to green (compromised $\Delta\psi_m$) mitochondria.

of the emitted light from 590 nm (orange) to 530 nm (green) (Williamson et al., 2010).

M-cadherin RNAi sensitizes C2C12 myoblasts to serum-starvation-induced apoptosis

To further explore the role of M-cadherin in regulating mitochondrial integrity and cell survival or apoptosis during myogenic differentiation, M-cadherin RNAi or control C2C12 myoblasts were cultured in serum-free medium. Mitochondria were isolated and $\Delta\psi_{mt}$ was assessed by JC-1 staining after 0, 6, 12, 24 or 48 hours of serum starvation. There was a transient decrease in the ratio of JC-1 orange to green staining of isolated mitochondria from all groups of cells in response to serum starvation, but the M-cadherin RNAi group had the lowest $\Delta\psi_{mt}$ at all time points compared with the control cells (Fig. 2A). These results show that knocking down M-cadherin by RNAi reduced $\Delta\psi_{mt}$ during serum starvation. The level of apoptotic DNA fragmentation was significantly increased in M-cadherin RNAi-treated cells that were still attached to the plates at all time points of serum starvation compared with the control groups (Fig. 2B). Furthermore, quantification of apoptotic cells from both attached and floating cell populations by TUNEL staining, demonstrated that there was a significant increase in the number of cells undergoing apoptosis during serum starvation in M-cadherin RNAi cells compared with the control groups (Fig. 2C). In addition, there were fewer cells that remained attached to the plates in the M-cadherin RNAi group compared with control groups when serum starvation progressed to longer time periods (supplementary material Fig. S1). Serum starvation caused an acute activation of caspase-9 in C2C12 myoblasts, which is indicative of activation of the mitochondrial-associated apoptotic pathway. The protein abundance of cleaved caspase-9 was significantly higher in M-cadherin RNAi cells at all time points of serum starvation compared with control untreated cells (supplementary material Fig. S2). This suggests that knockdown of M-cadherin expression sensitizes C2C12 myoblasts to serum-starvation-induced apoptosis.

M-cadherin-mediated signaling enhances PI3K/Akt-dependent inhibitory phosphorylation of Ser9 of GSK-3β

Akt is a key mediator of survival signaling pathways, and it is associated with cadherin signaling in various cells (De et al., 2009; Koutsouki et al., 2005). Because GSK-3β, another key regulator of cell fate and a phosphorylation target of Akt, is associated with muscle wasting, we also examined the change in GSK-3β phosphorylation in response to M-cadherin RNAi treatment in confluent cells. As a functional read-out for GSK-3β activation, the protein abundance of two targets for GSK-3β, cyclin D1 (Diehl et al., 1998) and survivin (Kaga et al., 2006) were measured. M-cadherin RNAi significantly reduced the activation of Akt in confluent C2C12 cells as determined by the expression of phosphorylated Akt Ser473 (Fig. 3A). Consequently, the inhibitory phosphorylation of GSK-3β Ser9 was decreased in M-cadherin RNAi cells. Quantification of the immunoblot signals from four independent experiments showed a statistically significant and a reproducible (bottom panel of Fig. 3A; supplementary material Fig. S4A,B) reduction in phosphorylated Akt Ser473, GSK-3β phosphorylation, survivin and cyclin D1 in C2C12 cells after M-cadherin RNAi. Conversely, the activation of M-cadherin-mediated signaling using a recombinant M-cadherin–Fc chimera induced a significant increase in phosphorylation of

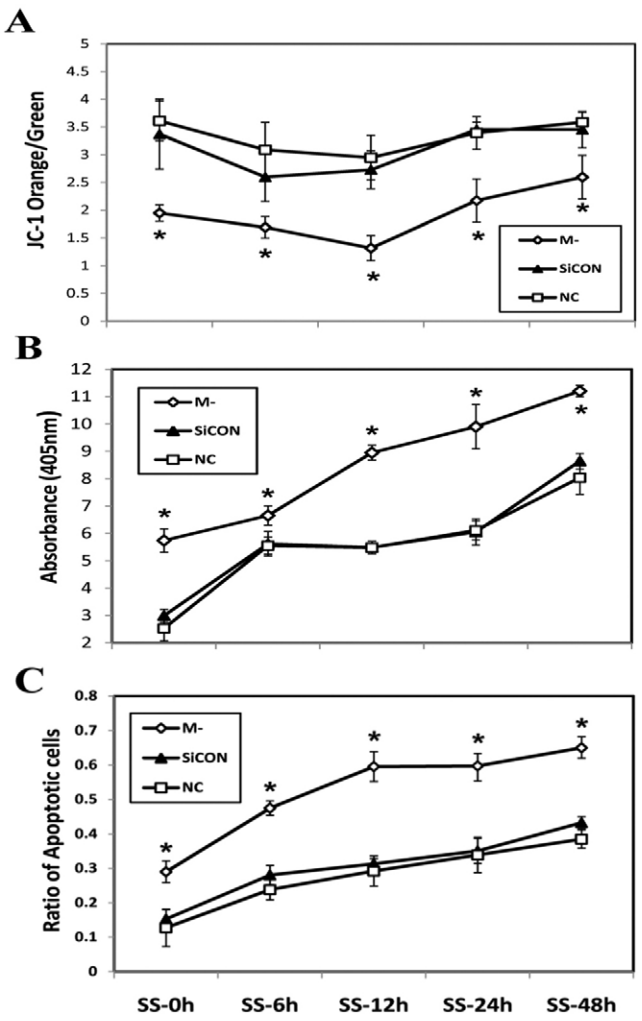

Fig. 2. Effect of M-cadherin RNAi on serum-starvation-induced apoptosis. M-cadherin RNAi (M-), non-targeted scrambled siRNA-transfected (SiCON) or normal control (NC) C2C12 myoblasts were serum starved from zero to 48 hours before being harvested. *$P<0.05$ vs both SiCON and NC control groups. The data are shown as the mean ± s.e.m. of three independent experiments. (**A**) Mitochondria were isolated from attached cells after serum starvation for 0 hours (SS-0h), 6 hours (SS-6h), 12 hours (SS-12h), 24 hours (SS-24h) or 48 hours (SS-48h). The mitochondria $\Delta\psi_m$ (orange to green ratio) was evaluated by FACS analysis of JC-1 staining. (**B**) DNA fragmentation in attached cells was measured by a cell death ELISA at the same time points as described in A. (**C**) The percentage of cells undergoing apoptosis in both attached and floating cells was defined as: (total TUNEL-positive attached cells + total TUNEL-positive floating cells)/(total attached cells + total floating cells).

Akt and GSK-3β at the corresponding residues (Fig. 3B; supplementary material Fig. S5A,B). The protein abundance of survivin and cyclin D1 decreased in response to suppression of M-cadherin by RNAi (Fig. 3A; supplementary material Fig. S4C,D). In addition, the protein abundance of survivin and cyclin D1 increased in response to rMFc treatment (Fig. 3B; supplementary material Fig. S5C,D). Immunoprecipitation data show that the binding between the p85α subunit of PI3K and M-cadherin was increased in response to treatment with recombinant M-cadherin–Fc chimera (Fig. 3C). The abundance of PI3K-p85α protein in the membrane fraction was markedly increased in M-cadherin–Fc-

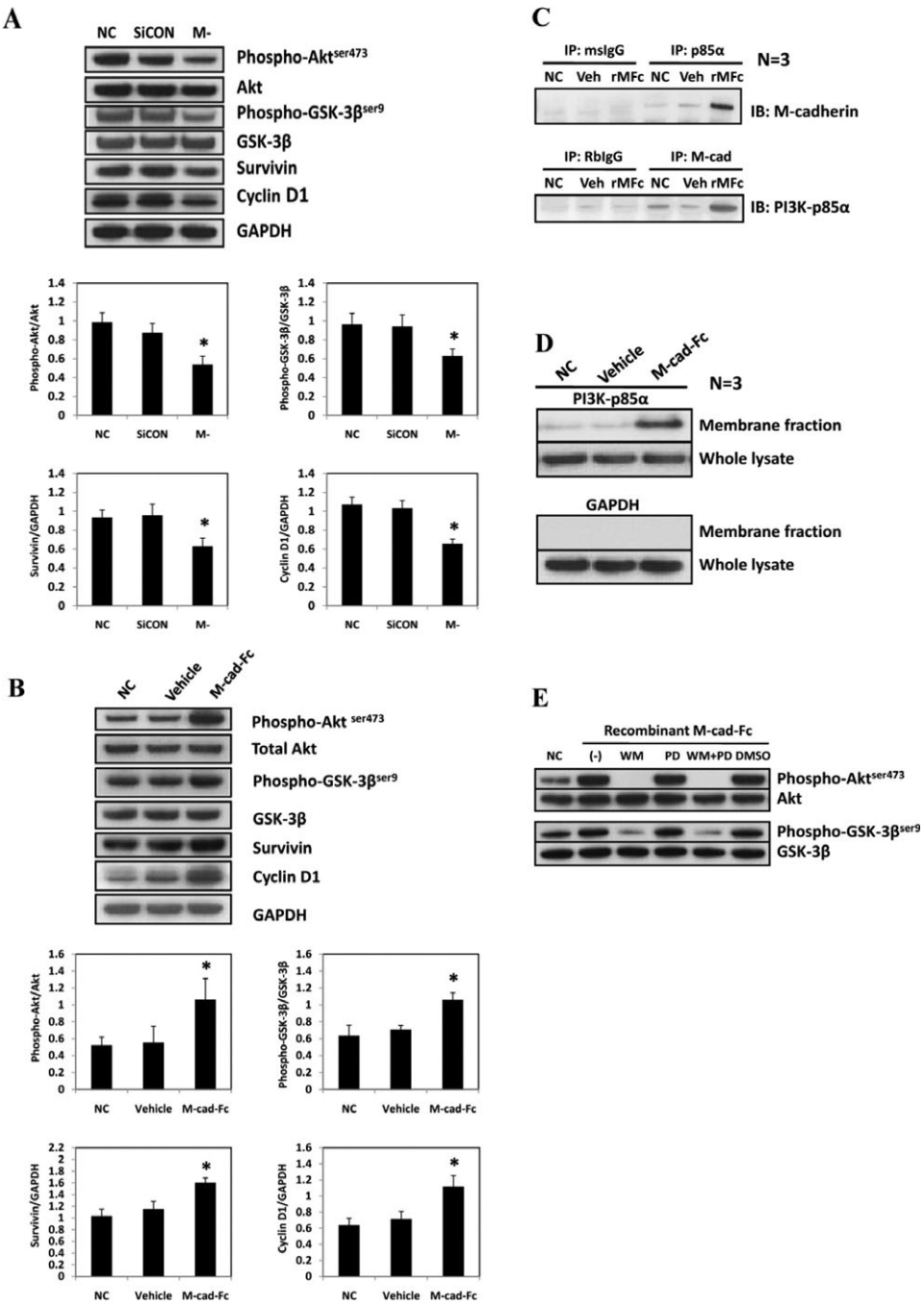

Fig. 3. M-cadherin-mediated signaling effect on the PI3K/Akt/GSK-3β pathway. (**A**) Representative immunoblots of M-cadherin-RNAi (M-) treated, non-targeted scrambled siRNA-transfected (SiCON) treated or normal control (NC) C2C12 cells (top). Survivin and cyclin D1 were measured as a functional read-out for GSK-3β activation. GAPDH was used as a loading control. Densitometric analyses of Akt, GSK-3β, survivin and cyclin D1 normalized to their loading controls (bottom). (**B**) C2C12 myoblasts were grown in normal control (NC), vehicle control (Vehicle) or recombinant M-cadherin–Fc-coated (M-cad–Fc) dishes for 48 hours (top). The cells were lysed and subjected to immunoblotting analysis of the same proteins as measured in Fig. 3A. Densitometric analyses of immunoblot band intensities of phosphorylated and total Akt and GSK-3β, as well as survivin and cyclin D1 in response to recombinant M-cadherin–Fc treatment (bottom). The band intensities of the above proteins were normalized by corresponding control proteins. (**C**) Immunoprecipitation assays of untreated C2C12 myoblasts (NC) or myoblasts treated with either the vehicle (Veh) or with recombinant M-cadherin–Fc (rMFc) were conducted 48 hours after incubation with either mouse anti-PI3K-p85α or rabbit anti-M-cadherin antibodies, respectively. Western blots of the protein abundance of M-cadherin or PI3K-p85α were conducted in the precipitated proteins. (**D**) Cell membrane fractions were prepared from cells that had been treated as described in C and blotted to detect the protein abundance of PI3K-p85α. (**E**) C2C12 myoblasts were treated as described in C. The cells were then treated for a subsequent 12 hours with no vehicle added (-), wortmannin (WM, 200nM), PD98059 (PD, 50 μM), wormannin plus PD98059 (WM+PD) or DMSO. Untreated normal control cells (NC) did not receive either the recombinant M-cadherin–Fc or the vehicle treatments. The cells were harvested for immunoblotting analysis. The data are shown as the mean ± s.e.m. of three independent experiments. *$P<0.05$ vs the control groups.

treated cells compared with the control cells (Fig. 3D). Treatment with the PI3K inhibitor, wortmannin, but not the MEK-1 inhibitor, PD9805, during the last 6 hours of M-cadherin–Fc treatment, completely prevented the increase in phosphorylated Akt Ser473 and phosphorylated GSK-3β Ser9. This shows that the increased inhibitory phosphorylation of GSK-3β that is induced by M-cadherin-mediated signaling, is PI3K dependent (Fig. 3E).

GSK-3β overexpression exacerbates, whereas M-cadherin–Fc treatment attenuates apoptosis induced by cell confluence or serum starvation

To further characterize the role of GSK-3β in regulating apoptosis, C2C12 myoblasts that were 80% confluent were transiently transfected with a wild-type GSK-3β plasmid and allowed to grow for 48 hours until they reached overconfluence. The transfection efficiency of the GSK-3β plasmid by FuGENE 6 in C2C12 cells was estimated to be ~20–30% (supplementary material Fig. S3A). Immunoblot analysis confirmed that transfection with GSK-3β increased the protein abundance of GSK-3β and also decreased the protein level of cyclin D1 (Fig. 4A), a target of GSK-3β phosphorylation that induces its degradation. Overexpression of wild-type GSK-3β in confluent C2C12 myoblasts increased the protein abundance of cleaved caspase-9, caspase-3 and PARP. This effect was reversed by co-treating the cells with recombinant M-cadherin–Fc (Fig. 4B,C). In addition, $\Delta\psi_{mt}$ was decreased in mitochondria from C2C12 cells upon overexpression of wild-type GSK-3β, which was rescued by co-treatment with recombinant M-cadherin–Fc (Fig. 4D). Together, these data indicate that overexpression of wild-type GSK-3β alone is sufficient to exacerbate the mitochondria-associated apoptosis induced by cell confluence, and this effect can be reversed by enhancement of M-cadherin-mediated signaling by treatment with M-cadherin–Fc. Furthermore, in response to serum starvation, cells transfected with wild-type GSK-3β plasmid had significantly higher cell death than

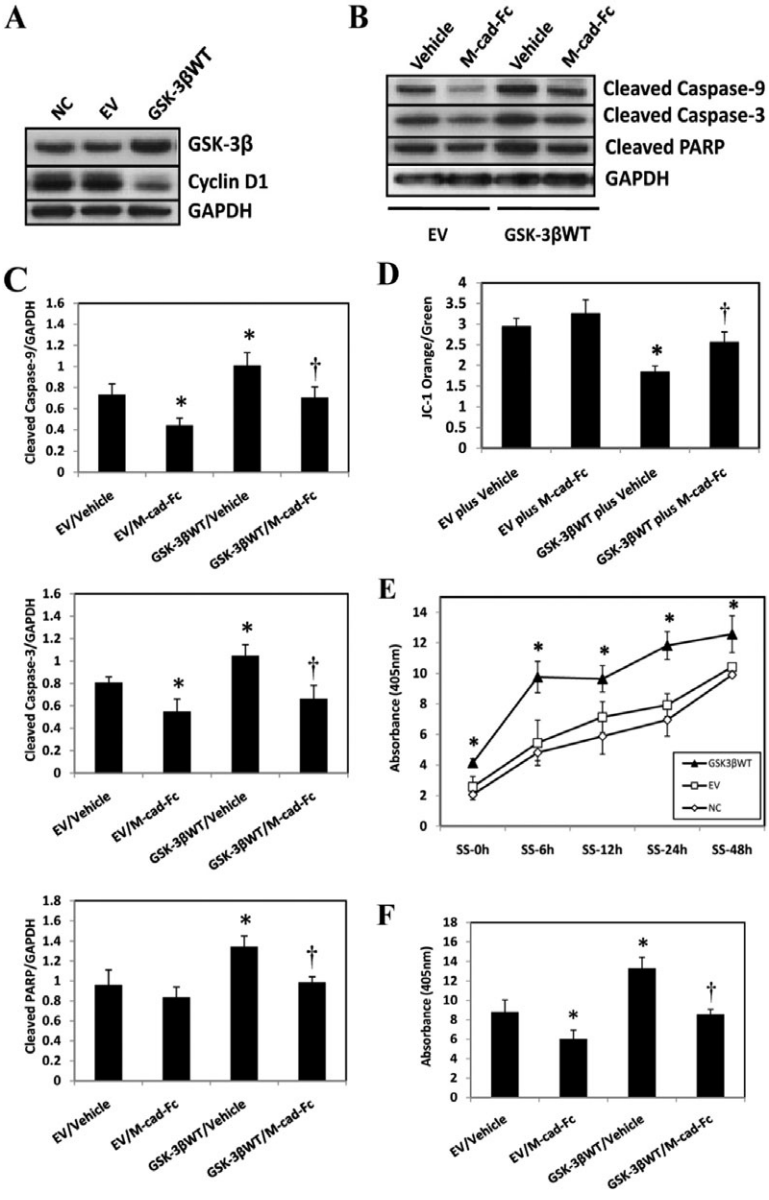

Fig. 4. Effect of wild-type GSK-3β overexpression and recombinant M-cadherin–Fc treatment on apoptosis induced by cell confluence or serum starvation. (**A**) A wild-type GSK-3β plasmid (GSK-3βWT) or an empty vector (EV) were transiently transfected into C2C12 myoblasts that were 80% confluent. 48 hours after transfection, cells were harvested in RIPA buffer and processed for immunoblotting for GSK-3β and cyclin D1 protein abundance. The experiment was repeated three times under each experimental condition. (**B**) Wild-type GSK-3β plasmids (GSK-3βWT) or empty vectors (EV) were transiently transfected into C2C12 myoblasts growing in recombinant M-cadherin–Fc-coated (M-cad-Fc) or vehicle-coated (Vehicle) dishes. 48 hours later, the cells were harvested in RIPA buffer and immunoblotted against pro-apoptotic proteins. GAPDH was probed as a loading control. (**C**) Densitometric analyses of immunoblot bands described in B. The data were normalized to GAPDH and expressed as the mean ± s.e.m. of three independent experiments. *$P<0.05$ vs EV/Vehicle or EV/M-cad-Fc. $^{\dagger}P<0.05$ vs GSK-3βWT/Vehicle. (**D**) Mitochondria were isolated from C2C12 myoblasts that had undergone the same treatments as described in B. The mitochondria were stained with JC-1. A FACSCalibur system was used to measure the change in mitochondrial membrane potential ($\Delta\psi_m$). The data are expressed as the ratio of orange to green JC-1 staining. The data are reported as the mean ± s.e.m. of three independent experiments. *$P<0.05$ vs EV/Vehicle or EV/M-cad-Fc. $^{\dagger}P<0.05$ vs GSK-3βWT/Vehicle. (**E**) C2C12 myoblasts transfected with the wild-type-GSK-3β plasmid (GSK3βWT) or the empty vector (EV) and the non-transfected normal control (NC) cells were serum-starved for 0 hours (SS-0h), 6 hours (SS-6h), 12 hours (SS-12h), 24 hours (SS-24h) or 48 hours (SS-48h). At the end of each time point, the attached cells were harvested and DNA fragmentation was measured by a cell death ELISA assay. The data represent the mean ± s.e.m. from three independent experiments. *$P<0.05$, vs NC or EV. (**F**) The wild-type GSK-3β plasmid (GSK3βWT) or the empty vector (EV) was transiently transfected into C2C12 myoblasts growing in recombinant M-cadherin–Fc-coated (M-cad-Fc) or vehicle-coated (Vehicle) dishes. 48 hours later, the cells were treated with serum starvation for another 48 hours before being harvested. A cell death ELISA assay was used to measure the DNA fragmentation in the harvested cells. The data represent the mean ± s.e.m. from three independent experiments. *$P<0.05$ vs EV/Vehicle or EV/M-cad-Fc. $^{\dagger}P<0.05$ vs GSK-3βWT/Vehicle.

the control cells at all time points, suggesting that overexpression of wild-type GSK-3β sensitized the cells to serum-starvation-induced apoptosis (Fig. 4E). By contrast, co-treatment of C2C12 cells with M-cadherin–Fc and GSK-3β overexpression after 48 hours of serum starvation significantly attenuated cell death, compared with GSK-3β overexpression alone (Fig. 4F).

GSK-3β inhibition attenuates apoptosis exacerbated by M-cadherin RNAi

The effect of GSK-3β inhibition on regulating apoptosis was examined using a myristoylated Akt mutant (myrAkt), which functions as a constitutively active form of Akt (Ahmed et al., 1997), to inhibit GSK-3β activity and a V5-tagged kinase-deficient mutant GSK-3β(K85R), which functions as a dominant-negative GSK-3β (Ma et al., 2008). The transfection efficiency of these plasmids using DharmaFECT Duo in C2C12 myoblasts was estimated to be 25-35% as determined from transfection studies using the pEGFP-C3 vector and DharmaFECT DUO as the transfection agent (supplementary material Fig. S3B).

To evaluate the effects of GSK-3β inhibition on apoptotic signaling, C2C12 cells that were 80% confluent were transfected with M-cadherin-targeted siRNA, plus either the myrAkt or the GSK-3β(K85R) plasmid, or an empty vector. The cells were allowed to grow for 48 hours at which time they had reached overconfluency. As expected, there was a significant increase in both phosphorylated Akt and total Akt abundance in the cells transfected with the myrAkt plasmid (Fig. 5A, right panel). In addition, there was an increase in total GSK-3β and cyclin D1 protein abundance in the cells that were transfected with GSK-3β(K85R) plasmids (Fig. 5A, left panel). Forced expression of myrAkt or GSK-3β(K85R) plasmids significantly attenuated apoptosis as seen by lower levels of cleaved caspase-9, cleaved caspase-3 and cleaved PARP (Fig. 5B,C) after M-cadherin RNAi or overconfluency. Furthermore, the DNA fragmentation that resulted from 48 hours of serum starvation or M-cadherin-targeted siRNA, was significantly reduced when the C2C12 cells were co-transfected with either myrAkt or GSK-3β(K85R) plasmids (Fig. 6A). To further confirm the impact of GSK-3β inhibition on the regulatory effect of M-cadherin on apoptosis, we transfected the cells with M-cadherin siRNA for 36 hours followed by treatment with a specific GSK-3 inhibitor TDZD-8 (20 μM) for 12 hours. TDZD-8 treatment abrogated apoptosis and reversed the loss of $\Delta\psi_{mt}$ that was caused by M-cadherin RNAi following a period of 48 hours of serum starvation (Fig. 6B,C).

GSK-3β inhibition partially restores the myogenic differentiation impaired by M-cadherin RNAi

Finally, we sought to investigate the impact of M-cadherin RNAi and GSK-3β inhibition on the outcome of myogenic differentiation. M-cadherin RNAi C2C12 myoblasts treated with

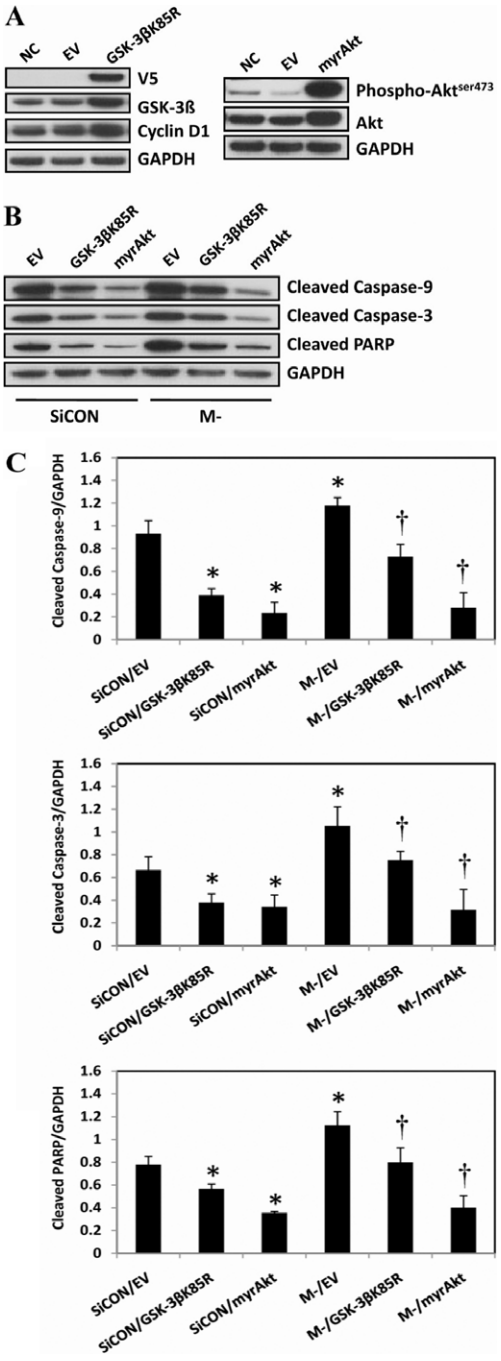

Fig. 5. Effect of GSK-3β inhibition on cell-confluence-induced apoptosis. (**A**) C2C12 myoblasts were grown to 80% confluency then transfected with an empty vector (EV) or GSK-3βK85R, which contained a V5 tag (left panel), or constitutively active Akt (myrAkt) (right panel) for 48 hours. Non-transfected cells normal control cells (NC) were cultured under identical conditions. The protein abundances of V5 tag, GSK-3β, and cyclin D1 were examined in cells transfected with GSK-3βK85R plasmid (left panel) and those of Ser437-phosphorylated and total Akt were examined in myrAkt plasmid-transfected cells (right panel) by immunoblotting. (**B**) C2C12 myoblasts were grown to 80% confluency then co-transfected with the M-cadherin-targeted siRNA (M-) plus myrAkt (M-/myrAkt) or the GSK-3βK85R plasmid (M-/GSK-3βK85R) or an empty vector (M-/EV). Similar co-transfections were completed with the non-targeted scramble siRNA (SiCON) with myrAkt (SiCON/myrAkt), GSK-3βK85R (SiCON/GSK-3βK85R) or the empty vector (SiCON/EV). 48 hours after transfection, the cells were harvested and processed for immunoblotting of cleaved caspase-9, cleaved caspase-3 and cleaved PARP. GAPDH was used as a loading control. Each experiment was repeated three times. (**C**) Densitometric analyses of immunoblots were obtained from C2C12 cells with identical treatments as described in Fig. 5B. The data represent the mean ± s.e.m. of three independent experiments. *$P<0.05$ vs SiCON/EV. †$P<0.05$ vs M-/EV.

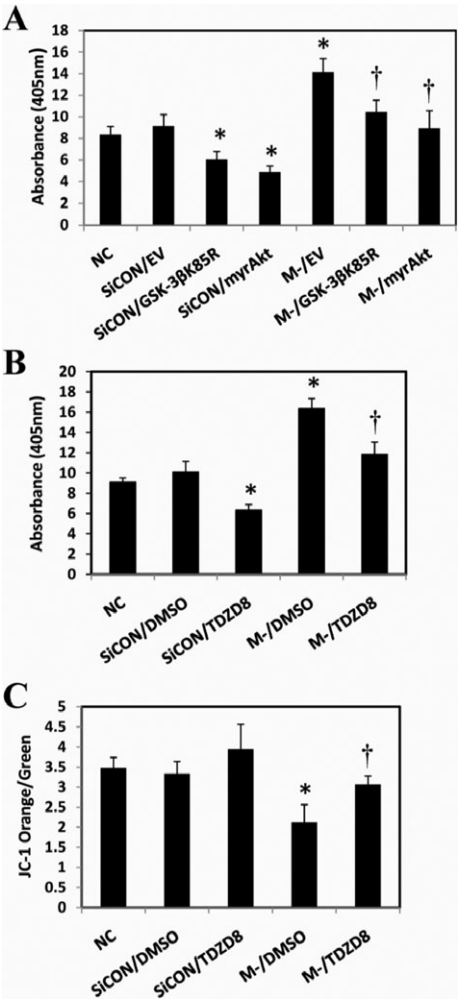

Fig. 6. Effect of GSK-3β inhibition on serum-starvation-induced apoptosis. (**A**) C2C12 cells were co-transfected with M-cadherin-targeted siRNA and one of the plasmids (myrAkt, GSK-3βK85R or empty vector) for 48 hours, then serum-starved for 48 hours. DNA fragmentation was measured by ELISA. $^{\dagger}P<0.05$ vs M-/EV. (**B**) C2C12 cells were transiently transfected with M-cadherin RNAi (M-), or a non-targeted scrambled siRNA (SiCON). These were compared with normal non-transfected C2C12 cells (NC). The cells were treated with 20 μM TDZD-8 or DMSO for the last 12 hours of siRNA transfection. 48 hours after transfection, the treated and control cells were serum starved for 48 hours. The cells were harvested and DNA fragmentation was assessed by cell death ELISA. Each experiment was repeated three times. $^{\dagger}P<0.05$ vs SiCON/TDZD8 and M-/DMSO. (**C**) Mitochondria were isolated from each experimental group and stained with JC-1. The ratio of JC-1 orange to green staining was analyzed using a FACSCalibur system to measure the mitochondrial membrane potential. $^{\dagger}P<0.05$ vs M-/DMSO. All experiments were repeated three times. $^{*}P<0.05$ vs NC or SiCON.

or without TDZD-8 were cultured in differentiation medium for 48 hours to induce myogenic differentiation. Immunofluorescent staining of myosin heavy chain (MyHC) was used as a terminal myogenic marker. A TUNEL assay was performed to determine the level of in situ apoptotic DNA fragmentation. Knockdown of M-cadherin by RNAi significantly impaired myogenic differentiation, because many cells died and detached from the plates. By contrast, TDZD-8 treatment partially restored the myogenic differentiation that was blocked by M-cadherin RNAi. This was determined by the myoblast fusion index, which represented the percentage of myoblasts that matured into myotubes (Fig. 7A,B). Calculation of the apoptotic index from TUNEL labeling showed that TDZD-8 treatment significantly attenuated the number of apoptotic nuclei that was caused by M-cadherin RNAi over 48 hours of myogenic differentiation (Fig. 7A,C).

These findings were further verified in mouse primary myoblasts. Syndecan-4-positive primary myoblasts were isolated by fluorescence-activated cell sorting (FACS) as representative muscle progenitor cells (Brack and Rando, 2007; Cornelison et al., 2001). About 20% of the adult muscle stem cells were syndecan-4 positive. Knockdown of M-cadherin by RNAi significantly impaired myotube formation from syndecan-4-positive primary myoblasts, which was partially rescued by TDZD-8 treatment as shown by MyHC staining and a greater fusion index (Fig. 8B,C) in the TDZD-8-treated cells. Furthermore, M-cadherin RNAi exacerbated apoptosis in syndecan-4-positive primary myoblasts after 48 hours of myogenic differentiation. Apoptosis could be abrogated by TDZD-8 treatment, as shown by reduced TUNEL staining (Fig. 8B) and a lower apoptotic index (Fig. 8D) after TDZD-8 treatment.

Discussion

This is the first report to show that M-cadherin-mediated signaling protects myoblasts against apoptosis during myogenic differentiation. In vitro culture of myoblasts at high cell density has been shown to yield not only a better myogenic differentiation outcome, but also an increased incidence of apoptosis, compared with culturing the cells at a low density (Dee et al., 2002). This observation is consistent with the suggestion that apoptosis and differentiation are tightly regulated in a coordinated pattern in myoblasts (Walsh, 1997). In the current study, we show that M-cadherin protein abundance is increased and M-cadherin engagement at cell–cell contacts is induced when myoblasts become confluent. Although confluence triggers apoptosis during differentiation, other cells survive, differentiate and fuse into myotubes (Allombert-Blaise et al., 2003; Dee et al., 2002; Fernando and Megeney, 2007; Lippens et al., 2005; Walsh, 1997).

In this study, we showed that the disruption of M-cadherin signaling by M-cadherin RNAi, sensitized C2C12 myoblasts to apoptosis that was induced by either cell confluence or serum starvation. Apoptosis in C2C12 cells is accompanied by decreased $\Delta\psi_{mt}$, increased mitochondrial release of cytochrome *c* and AIF, and consequently, increased cleavage of caspase-9 but not caspase-8. Together, these data indicate that apoptosis induced by M-cadherin RNAi is mediated by the intrinsic mitochondria-associated pathway, and that M-cadherin-mediated signaling plays an important role in maintaining the mitochondrial integrity of differentiating myoblasts and suppressing apoptosis during myogenic differentiation. Our findings are consistent with data showing that $\Delta\psi_{mt}$ is compromised in myoblasts undergoing apoptosis, but not those that successfully differentiate (van den Eijnde et al., 2001). Furthermore, proper mitochondria function is crucial for successful myogenic differentiation (Jahnke et al., 2009; Rochard et al., 1996; Rochard et al., 2000).

Previous findings have shown that in aged muscle, the number of M-cadherin-positive satellite cells is decreased (Sajko et al., 2004), but the apoptotic propensity of satellite cells is increased

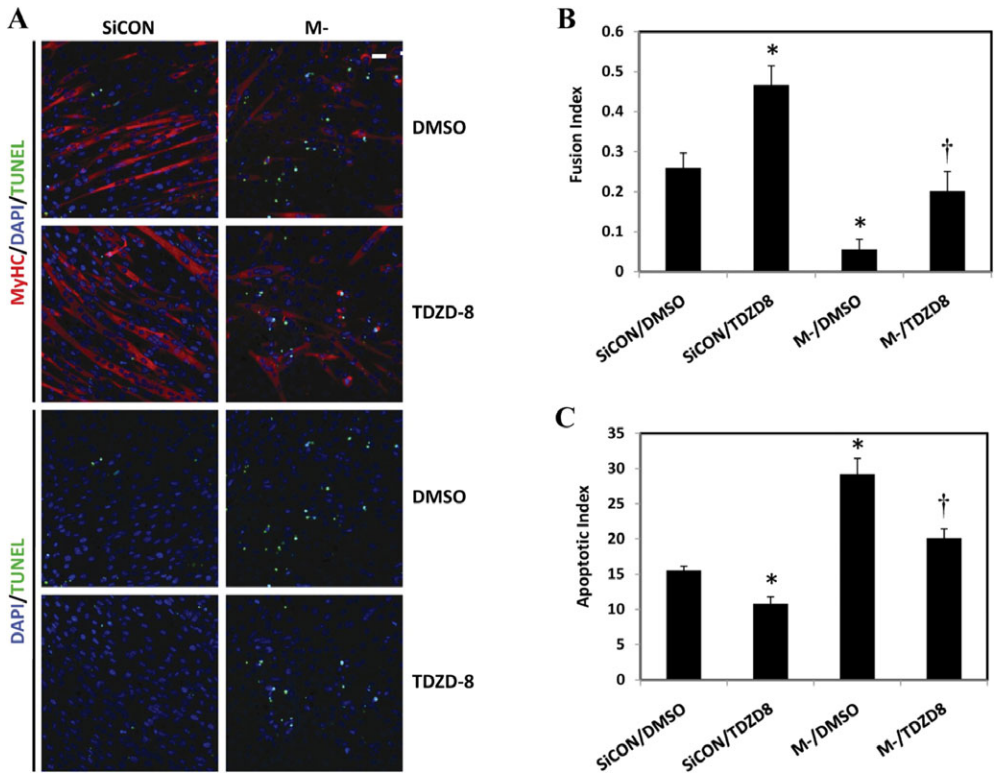

Fig. 7. Effect of M-cadherin RNAi and GSK-3β inhibition on myogenic differentiation of C2C12 myoblasts. C2C12 cells were grown on coverslips, transfected with M-cadherin-targeted (M-) or non-targeted scrambled siRNA (SiCON) for 36 hours then incubated with or without TDZD-8 for 12 hours. The cells were then cultured in differentiation medium for 48 hours. (**A**) Representative confocal images of C2C12 myoblasts after treatment with a combination of M-cadherin RNAi (M-) or non-targeted scrambled siRNA transfection (SiCON) and TDZD-8 or DMSO as a vehicle control. The cells were cultured in differentiation medium for 48 hours after the co-treatments. MyHC, red; DAPI, blue; TUNEL, green. Scale bar: 100 μm. (**B**,**C**) Data from three independent experiments as mean ± s.e.m. *$P<0.05$ vs SiCON/DMSO; $^{\dagger}P<0.05$ vs M-/DMSO. The myoblast fusion index was calculated for cells after each treatment described in Fig. 7A, as the ratio of the number of DAPI-positive nuclei located in the MyHC-positive myotubes (i.e., fused myoblasts) divided by the total number of nuclei in the same field (B). The apoptotic index was calculated as the percentage of total nuclei that were TUNEL positive (C).

compared with those in young animals (Jejurikar et al., 2006; Jejurikar and Kuzon, Jr, 2003). This suggests that there is a negative relationship between the expression levels of M-cadherin and the apoptosis susceptibility of muscle progenitor cells. In the current study, we showed that M-cadherin has a protective role against apoptosis during myogenic differentiation because inhibition of M-cadherin expression by RNAi, sensitized both C2C12 and syndecan-4-positive primary myoblasts to apoptosis, which resulted in an increase in pro-apoptotic markers and in impaired myotube formation compared with levels in control cells. We speculate that reduced M-cadherin might be a contributing mechanism that would explain, at least in part, a increased susceptibility of muscle progenitor cells to increased apoptotic signaling and elimination of nuclei in aged muscles (Alway et al., 2011; Alway and Siu, 2008; Jejurikar et al., 2006; Jejurikar and Kuzon, Jr, 2003).

GSK-3β is a serine-threonine kinase that is constitutively active in resting cells and plays a key role in regulating glucose homeostasis (Frame and Cohen, 2001). GSK-3β is also important in regulating apoptosis. However, it has a paradoxical effect on apoptosis from different pathways by promoting mitochondrial-dysfunction-associated apoptosis signaling, but also inhibiting death-receptor-mediated apoptosis signaling (Beurel and Jope, 2006). Dysregulation of GSK-3β has been reported to be involved in several pathologies, including neurodegenerative diseases, mood disorders, cancer and diabetes (Beurel and Jope, 2006). Studies in skeletal muscles have linked GSK-3β to muscle-wasting conditions. GSK-3β activity has been shown to increase in aged (Kinnard et al., 2005) and burn-injured skeletal muscles (Fang et al., 2007). Inhibition of GSK-3β is required for IGF-1-induced myogenic differentiation (Vyas et al., 2002). Furthermore, GSK-3β inhibition reduces protein degradation in conditions of muscle wasting and might also promote re-growth of atrophic muscle (Evenson et al., 2005; van der Velden et al., 2006; van der Velden et al., 2007). Although a conditional skeletal muscle knockout of GSK-3β has been reported to manifest a phenotype with an improved insulin tolerance and glucose metabolism in muscle tissues (Patel et al., 2008), currently, there are no data that evaluate a direct role of GSK-3β in regulating the muscle progenitor cell survival and apoptosis during myogenic differentiation. In this study, we show for the first time that overexpression of wild-type GSK-3β is sufficient to induce apoptosis in confluent C2C12 myoblasts and to sensitize the cells to serum-starvation-induced apoptosis. This effect can be attenuated by increasing M-cadherin-mediated signaling by recombinant M-cadherin–Fc treatment. We also

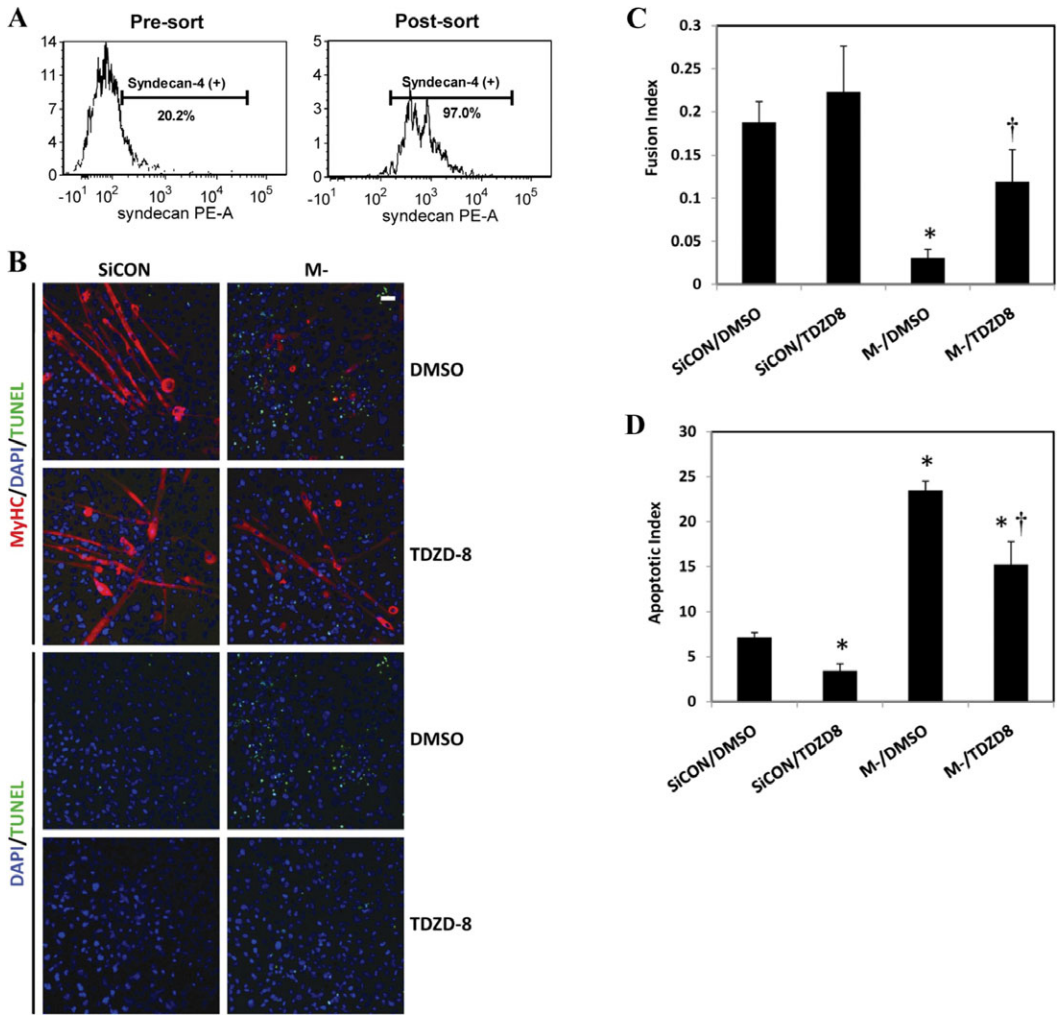

Fig. 8. Effect of M-cadherin RNAi and GSK-3β inhibition on apoptosis and myogenic differentiation of primary syndecan-4-positive myoblasts. Primary myoblasts were isolated from hindlimb muscles of 1-week-old C57BL/6 mice and syndecan-4-positive myoblasts were purified from isolated cells by fluorescence activated cell sorting (FACS). (**A**) Approximately 20.2% cells of adult stem cells that were isolated from hindlimb skeletal muscles were syndecan-4 positive (left). The post-sort verification of FACS sorted cells indicated that the purity of syndecan-4-positive cells was 97% (right). (**B**) Syndecan-4-positive myoblasts were grown on coverslips and treated as described in Fig. 7. The imaging of the cells was the same as in Fig. 7A. (**C**,**D**) Data from three independent experiments were given as mean ± s.e.m. *$P<0.05$ vs SiCON/DMSO. †$P<0.05$ vs M-/DMSO. (**C**) The myoblast fusion index was calculated as described in Fig. 7B. (**D**) The apoptotic index was calculated as described in Fig. 7C.

show that the activation of M-cadherin-mediated signaling recruits PI3K and activates Akt, which in turn phosphorylates GSK-3β at the Ser9 residue, resulting in its suppression. Conversely, inhibition of GSK-3β activation attenuates apoptosis that is induced by knockdown of M-cadherin expression. This suggests that GSK-3β plays a crucial role in mediating the protective effect of M-cadherin against apoptosis during myogenic differentiation. Our findings are consistent with data from Robakis and colleagues (Baki et al., 2004) who showed that the expression of presenilin-1 in fibroblasts promotes the association of PI3K with E- and N-cadherins and activates Akt, leading to the inhibition of GSK-3β activity. Skeletal muscle is the largest consumer of glucose, and GSK-3β plays an important role in regulating glucose metabolism and insulin sensitivity in muscle (Patel et al., 2008; Pearce et al., 2004). Thus we speculate that manipulation of M-cadherin-mediated cell–cell adhesion might have a profound impact on glucose metabolism and insulin tolerance of muscle tissue through regulating the activation status of GSK-3β. Interestingly, a type 2 diabetic phenotypic KK/Ta mouse, has been shown to have an ectopic expression of M-cadherin with three missense mutations in liver (Shiina et al., 2007). Further statistical analysis revealed a correlation between M-cadherin expression and the hypertriglyceridemia, glucose intolerance and hyperinsulinemia in the KK/Ta mouse. This suggests that disrupted M-cadherin signaling might have a role in the pathology of type 2 diabetes (Shiina et al., 2007).

GSK-3β might regulate mitochondrial outer membrane permeabilization by targeting multiple substrates. The Bcl-2 family of proteins represents one target of GSK-3β. GSK-3β directly phosphorylates the pro-apoptotic Bax protein at Ser163, leading to its activation (Linseman et al., 2004). GSK-3β activation also induces the expression of the pro-apoptotic Bim

protein (Hongisto et al., 2003). However, GSK-3β phosphorylation of MCL-1, an anti-apoptotic member of Bcl-2 family protein, facilitates its degradation (Maurer et al., 2006). Another class of GSK-3β substrates in regulating apoptosis is a group of transcription factors that include p53, β-catenin and Myc. p53 plays a crucial role in regulating cell cycle arrest, senescence and apoptosis. GSK-3β can form a complex with nuclear p53 and this promotes p53-induced apoptosis (Watcharasit et al., 2003). β-catenin is a key mediator for the canonical Wnt signaling pathway, which has an important role in promoting cell growth and survival. β-catenin also connects cadherins to the actin cytoskeleton. Together with adenomatous polyposis coli (APC) and axin, GSK-3β forms the 'destruction complex' that phosphorylates β-catenin and promotes its ubiquitylation and degradation (Ewan et al., 2010). Cadherins control both the turnover rate and the subcellular distribution of β-catenin. As a result, β-catenin could be the nexus for the convergence of cadherin and GSK-3β-mediated signaling in skeletal muscle. Additional studies are required to identify the important upstream mediators and downstream targets for M-cadherin–Akt–GSK-3β signaling that are responsible for maintaining mitochondrial integrity and suppressing apoptosis in myoblasts; however, this is beyond the scope of the current investigation.

In conclusion, the data in the current study show that M-cadherin plays a critical role in regulating survival versus death by apoptosis of myoblasts during myogenic differentiation in vitro. M-cadherin-mediated signaling maintains the inhibitory tone from PI3K–Akt upon GSK-3β by activating PI3K–Akt. M-cadherin signaling appears to help maintain a balance between apoptosis and differentiation and prevents the acceleration of mitochondrial-associated apoptotic signaling in muscle cells.

Materials and Methods

Cell culture

C2C12 myoblasts were purchased from American Type Culture Collection (Manassas, VA) and maintained in Dulbecco modified Eagle's medium (DMEM) (Invitrogen Life Technologies, Bethesda, MD) supplemented with 10% fetal bovine serum (FBS) and 1% antibiotic and antimycotic mixture solution (Invitrogen).

Primary myoblasts were isolated from hindlimb muscles of one-week old C57BL/6 mice (Goodell et al., 2001) and purified by Percoll (Sigma, St Louis, MO) gradient centrifugation. The syndecan-4-positive myoblasts were identified by fluorescence-activated cell sorting (FACS) using an antibody against syndecan-4 (BD). The Syndecan-4-positive myoblasts were cultured in Ham's F10 supplemented with 20% FBS at 37℃.

Serum starvation was induced by incubating the cells in serum-free DMEM supplemented with 1% antibiotic and antimycotics. Myogenic differentiation was induced by culturing the confluent cells in differentiation medium (DMEM, 2% horse serum, 1% antibiotic and antimycotic).

Chemical inhibitors

The cells were treated with the PI3K inhibitor wortmannin (200 nM, Alexis Biochemicals, Plymouth Meeting, PA), the GSK-3 inhibitor TDZD-8 (25 μM, Sigma) or the MEK1 inhibitor PD98059 (50 μM, Cell Signaling, Danvers, MA).

Inhibition of M-cadherin expression by RNA interference

The myoblasts were seeded at a density of 1.7×10^5 per well in a six-well plate, 24 hours before transfection with SMARTpool small interfering RNA (siRNA) targeted to M-cadherin mRNA (Life Thermo). The transfection medium included either DharmaFECT-3 reagent (Life Thermo) (for C2C12 myoblasts) or Lipofectamine 2000 (Invitrogen) (for primary myoblasts) at a final siRNA duplex concentration of 100 nM. The efficacy of M-cadherin protein knockdown by RNAi was confirmed by immunoblotting (supplementary material Fig. S2).

Plasmids and transfection

The full-length mouse wild-type GSK-3β cDNA was generated by RT-PCR. mRNA was derived from wild C2C12 myoblasts using Trizol reagent (Life Technologies) and reverse-transcribed into cDNA using Superscript II (Life Technologies). The PCR product was cloned into the expression vector pcDNA3.1/myc-His(-) (Invitrogen). The constitutively active mutant of Akt (myrAkt) and the V5-tagged kinase-deficient GSK-3β mutant (K85R) carried by vector pcDNA3 were generous gifts from Jia Luo, University of Kentucky, Lexington, KY. The cells were transfected with the wild-type GSK-3β plasmids using FuGENE 6 (Roche Diagnostics, Indianapolis, IN). The co-transfection of siRNA against M-cadherin with myrAkt or GSK-3β (K85R) plasmids was carried out using DharmaFECT Duo transfection reagent (Dharmacon, Thermo-Fisher Scientific, Lafayette CO).

Recombinant M-cadherin–Fc treatment

The recombinant M-cadherin–Fc chimera was purchased from R&D Systems (Minneapolis, MN). Six-well plates were pre-coated with goat anti-Fc antibody (0.5 μg/cm^2 in PBS with Ca^{2+}; Jackson ImmunoResearch, West Grove, PA) overnight at 4℃ followed by coating with recombinant M-cadherin–Fc chimera at a final concentration of 2 μg/cm^2 in 0.1% BSA in PBS with Ca^{2+} for 2 hours at room temperature. The dishes were blocked with 1% BSA in HBSS with Ca^2. Plates coated with only the anti-Fc antibody were used as vehicle controls. The cells were seeded at 0.5×10^5 cells per well and grown for 48 hours before being harvested for further assays.

Subcellular fractionation

The membrane fraction of C2C12 myoblasts was prepared using a commercial reagent (Thermo Fisher). The nuclear protein fraction was prepared according to methods that have been previously described (Siu and Alway, 2005). The mitochondrial, mitochondria-free and nuclei-free cytosolic fractions were prepared using mitochondria and cytosol reagents (BioVision, Mountain View, CA). The concentration of the protein extracts was quantified in duplicate by Bio-Rad DC Protein Assay (BioRad, Hercules, CA). The whole-cell lysate was obtained by disrupting the cells with RIPA buffer supplemented with protease and phosphatase inhibitor cocktails (Sigma, 1:100 dilution) followed by centrifugation. The supernatant was collected as the whole-cell lysate.

Immunoblotting

Antibodies specific to phosphorylated Ser473 Akt, total Akt, phosphorylated Ser9 GSK3β, total GSK3β, cytochrome *c*, cleaved caspase-9 and cleaved caspase-3, AIF, survivin (1:1000) and cyclin D1 (1:2000 dilution) were purchased from Cell Signaling Technology (Danvers, MA). The anti-M-cadherin antibody (1:200) was obtained from Calbiochem (La Jolla, CA). The anti-caspase-8 antibody (1:250) was purchased from Santa Cruz Biotechnology (Santa Cruz, CA). Anti-histone H2B (1:5000), -β-tubulin (1:500) and anti-GAPDH (1:5000) were obtained from Abcam (Cambridge, MA). The antibodies against manganese superoxide dismutase (MnSOD) and copper-zinc superoxide dismutase (Cu-ZnSOD) (1:1000) were purchased from Millipore (Billerica, MA). The secondary antibodies for immunoblotting including goat anti-rabbit or goat anti-mouse IgG conjugated with horseradish peroxidase (HRP) were obtained from Jackson ImmunoResearch Laboratories (West Grove, PA). The proteins were separated on a 4–12% gradient polyacrylamide gel (Invitrogen), and transferred to a nitrocellulose membrane (Bio-Rad). The membranes were probed with primary antibodies overnight at 4℃, followed by incubation of the appropriate secondary antibody for 1 hour at room temperature. The resulting signals were developed using an enhanced chemiluminescence lighting (ECL) western blotting detection reagent kit (GE Health Care, Piscataway, NJ). Digital records were obtained from each blot and the protein bands of interest were quantified using 1D analysis software (Eastman Kodak). The membranes were stripped and reprobed for β-tubulin, GAPDH or histone H2B as loading controls.

Immunoprecipitation

The cells were washed in ice-cold PBS and lysed in ice-cold buffer (150 mM NaCl, 50 mM Tris-HCl, pH 7.5, 0.25% SDS, 0.1% Nonidet P-40). Non-soluble materials were removed by centrifugation at 12,000 ***g***. The lysate was incubated with anti-PI3K-p85α (Abcam), anti-M-cadherin (Santa Cruz) or IgG (Millipore) overnight at 4℃. The sample was then incubated with Protein A/G PLUS-agarose beads (Santa Cruz) and the beads were then collected by centrifugation. The bound proteins were eluted from the agarose beads in 5× Laemmli sample buffer at 95–100℃. The samples were clarified by centrifugation and the supernatants were separated by SDS-PAGE and immunoblotted against M-cadherin or PI3K-p85α.

Cell imaging

Phase-contrast images of live C2C12 and primary myoblast cells were obtained by a Nikon Eclipse TS100 phase-contrast microscope equipped with 10× 0.25 NA and 20× 0.40 NA phase-contrast objectives. The digital images were obtained with a SPOT RT camera and analyzed with SPOT RT software (Diagnostic Instruments, Sterling Heights, MI). Immunocytochemical assays were conducted on fixed cells after they had been grown on coverslips. After fixation in 4% paraformaldehyde, the cells were incubated at 4℃ with antibodies against anti-M-cadherin (1:20, Calbiochem) or anti-myosin heavy chain (MyHC) (1:500,

Developmental Studies Hybridoma Bank, Iowa City, IA). The cells were incubated with the Alexa Fluor 546 IgG (H+L) (Invitrogen) and counterstained with 4,6-diamidino-2-phenylindole (DAPI). The cells were imaged with a Zeiss LSM510 confocal laser-scanning microscope using AIM software (Carl Zeiss MicroImaging).

Myoblast fusion index

The myoblast fusion index was calculated as the ratio of the number of DAPI-positive nuclei located in the MyHC-positive myotubes (i.e. fused myoblasts) divided by the total number of nuclei in the same field. This fusion index was used as a read-out of myogenic differentiation. The fusion index was obtained from 10 non-overlapping areas of each coverslip.

Apoptosis assays

DNA fragmentation

DNA fragmentation was used to assess the level of apoptosis in muscle cells using an ELISA (Roche) with measurements for DNA fragmentation that were made at an absorbance of 405 nm (Siu et al., 2009; Siu and Alway, 2005). The data were normalized to the protein concentration of the sample.

Terminal deoxynucleotidyl transferase dUTP nick end labeling (TUNEL)

A TUNEL assay (Roche) was used to identify the extent of apoptotic nuclei in adherent myoblasts as reported previously (Siu et al., 2005b). The nuclei of all cells were counter-stained with DAPI. The number of TUNEL- and DAPI-positive nuclei was counted in ten images from non-overlapping areas of each group of cells. The data were presented as the apoptosis index, which was determined by the ratio of TUNEL-positive nuclei to the total number of DAPI-positive nuclei.

Because treatment with serum starvation and M-cadherin-siRNA resulted in apoptosis and cell death, some cells detached from the plates. To identify the full extent of apoptosis, and determine whether M-cadherin RNAi increased the sensitivity of C2C12 myoblasts to serum-starvation-induced apoptosis, we assessed apoptosis by a TUNEL assay in both adherent and floating cells in each well using published methods (Dee et al., 2002). The total percentage of apoptotic cells for each well was calculated as: (total number of TUNEL-positive attached cells + the total number of TUNEL-positive floating cells) /(total attached cells + total floating cells).

Cardiolipin content and mitochondrial membrane potential measurement

Nonyl acridine orange (NAO, Invitrogen) was used to determine the cardiolipin content in the inner mitochondrial membrane as an indicator of mitochondrial integrity. C2C12 myoblasts were transfected with M-cadherin-targeted (M-) or scrambled siRNA (siCON) with NAO (250nM) at 37°C. Fluorescence was visualized with a Nikon eclipse E800 fluorescence microscope and digital images were captured using a SPOT RT camera (Diagnostic Instruments). The fluorescence intensity was analyzed and quantified using the ImageJ software (NIH).

To measure changes in the mitochondrial membrane potential, mitochondria were isolated from M-cadherin RNAi or control cells and incubated with MitoTracker Deep Red 633 (Molecular Probes, Carlsbad, CA), a mitochondria-specific marker and analyzed by flow cytometry. This fluorescent dye diffuses passively into intact and respiring mitochondria. The mitochondrial membrane potential ($\Delta\psi_{mt}$) was estimated by staining the mitochondria with 5,5′,6,6′-tetrachloro-1,1′,3,3′-tetraethylbenzimidazolylcarbocyanine iodide (JC-1) (Molecular Probes). The staining results of JC-1 orange/green were analyzed using a FACSCalibur system (BD Bioscience) using Cell Quest Pro. 4.0 Software. 100,000 gated events were collected for each sample.

Statistical analyses

The results are presented as mean ± s.e.m. Statistical analyses were performed using the SPSS 13.0 software package. A one-way analysis of variance (ANOVA) was used to compare differences in all measured variables. $P<0.05$ was considered statistical significant.

Acknowledgements

We thank Jia Luo (University of Kentucky) for generously providing the Akt and GSK-3β plasmids and Yong Qian (National Institute of Occupational Safety and Health) for kindly providing the EGFP-C3 vector. We would like to acknowledge the assistance of Karen H. Martin, Kathleen M. Brundage and Christopher F. Cuff.

Funding

The West Virginia University Flow Cytometry core facility was supported by the National Institutes of Health [grant number, 5P20RR016440 subcontract 6544] to C.F.C. The West Virginia University Microscope Imaging Facility was supported by the Mary Babb Randolph Cancer Center and the National Institutes of Health [grant number 5P20RR016440-09] to L. F. Gibson. This work was supported by the National Institutes of Health [grant number, R01AG021530] to S.E.A. Deposited in PMC for release after 12 months.

Supplementary material available online at
http://jcs.biologists.org/lookup/suppl/doi:10.1242/jcs.086686/-/DC1

References

Adams, J. M. (2003). Ways of dying: multiple pathways to apoptosis. *Genes Dev.* **17**, 2481-2495.

Ahmed, N. N., Grimes, H. L., Bellacosa, A., Chan, T. O. and Tsichlis, P. N. (1997). Transduction of interleukin-2 antiapoptotic and proliferative signals via Akt protein kinase. *Proc. Natl. Acad. Sci. USA* **94**, 3627-3632.

Allombert-Blaise, C., Tamiji, S., Mortier, L., Fauvel, H., Tual, M., Delaporte, E., Piette, F., DeLassale, E. M., Formstecher, P., Marchetti, P. et al. (2003). Terminal differentiation of human epidermal keratinocytes involves mitochondria- and caspase-dependent cell death pathway. *Cell Death. Differ.* **10**, 850-852.

Alway, S. E., Morissette, M. R. and Siu, P. M. (2011). Aging and apoptosis in muscle. In *Handbook of the Biology of Aging*, 7th edn (ed. E. J. Masoro and S. Austad), pp. 63-118. Amsterdam: Elsevier.

Alway, S. E. and Siu, P. M. (2008). Nuclear apoptosis contributes to sarcopenia. *Exerc. Sport Sci. Rev.* **36**, 51-57.

Baehrecke, E. H. (2002). How death shapes life during development. *Nat. Rev. Mol. Cell Biol.* **3**, 779-787.

Baki, L., Shioi, J., Wen, P., Shao, Z., Schwarzman, A., Gama-Sosa, M., Neve, R. and Robakis, N. K. (2004). PS1 activates PI3K thus inhibiting GSK-3 activity and tau overphosphorylation: effects of FAD mutations. *EMBO J.* **23**, 2586-2596.

Beurel, E. and Jope, R. S. (2006). The paradoxical pro- and anti-apoptotic actions of GSK3 in the intrinsic and extrinsic apoptosis signaling pathways. *Prog. Neurobiol.* **79**, 173-189.

Brack, A. S. and Rando, T. A. (2007). Intrinsic changes and extrinsic influences of myogenic stem cell function during aging. *Stem Cell Rev.* **3**, 226-237.

Charrasse, S., Comunale, F., Grumbach, Y., Poulat, F., Blangy, A. and Gauthier-Rouviere, C. (2006). RhoA GTPase regulates M-cadherin activity and myoblast fusion. *Mol. Biol. Cell* **17**, 749-759.

Charrasse, S., Comunale, F., Fortier, M., Portales-Casamar, E., Debant, A. and Gauthier-Rouviere, C. (2007). M-cadherin activates Rac1 GTPase through the Rho-GEF trio during myoblast fusion. *Mol. Biol. Cell* **18**, 1734-1743.

Collins, C. A., Zammit, P. S., Ruiz, A. P., Morgan, J. E. and Partridge, T. A. (2007). A population of myogenic stem cells that survives skeletal muscle aging. *Stem Cells* **25**, 885-894.

Conboy, I. M., Conboy, M. J., Wagers, A. J., Girma, E. R., Weissman, I. L. and Rando, T. A. (2005). Rejuvenation of aged progenitor cells by exposure to a young systemic environment. *Nature* **433**, 760-764.

Corbu, A., Scaramozza, A., Badiali-DeGiorgi, L., Tarantino, L., Papa, V., Rinaldi, R., D'Alessandro, R., Zavatta, M., Laus, M., Lattanzi, G. et al. (2010). Satellite cell characterization from aging human muscle. *Neurol. Res.* **32**, 63-72.

Cornelison, D. D., Filla, M. S., Stanley, H. M., Rapraeger, A. C. and Olwin, B. B. (2001). Syndecan-3 and syndecan-4 specifically mark skeletal muscle satellite cells and are implicated in satellite cell maintenance and muscle regeneration. *Dev. Biol.* **239**, 79-94.

Day, K., Shefer, G., Shearer, A. and Yablonka-Reuveni, Z. (2010). The depletion of skeletal muscle satellite cells with age is concomitant with reduced capacity of single progenitors to produce reserve progeny. *Dev. Biol.* **340**, 330-343.

De, S. G., Miotti, S., Mazzi, M., Canevari, S. and Tomassetti, A. (2009). E-cadherin directly contributes to PI3K/AKT activation by engaging the PI3K-p85 regulatory subunit to adherens junctions of ovarian carcinoma cells. *Oncogene* **28**, 1206-1217.

Dee, K., Freer, M., Mei, Y. and Weyman, C. M. (2002). Apoptosis coincident with the differentiation of skeletal myoblasts is delayed by caspase 3 inhibition and abrogated by MEK-independent constitutive Ras signaling. *Cell Death. Differ.* **9**, 209-218.

Diehl, J. A., Cheng, M., Roussel, M. F. and Sherr, C. J. (1998). Glycogen synthase kinase-3beta regulates cyclin D1 proteolysis and subcellular localization. *Genes Dev.* **12**, 3499-3511.

Evenson, A. R., Fareed, M. U., Menconi, M. J., Mitchell, J. C. and Hasselgren, P. O. (2005). GSK-3beta inhibitors reduce protein degradation in muscles from septic rats and in dexamethasone-treated myotubes. *Int. J. Biochem. Cell Biol.* **37**, 2226-2238.

Ewan, K., Pajak, B., Stubbs, M., Todd, H., Barbeau, O., Quevedo, C., Botfield, H., Young, R., Ruddle, R., Samuel, L. et al. (2010). A useful approach to identify novel small-molecule inhibitors of Wnt-dependent transcription. *Cancer Res.* **70**, 5963-5973.

Fang, C. H., Li, B., James, J. H., Yahya, A., Kadeer, N., Guo, X., Xiao, C., Supp, D. M., Kagan, R. J., Hasselgren, P. O. et al. (2007). GSK-3beta activity is increased in skeletal muscle after burn injury in rats. *Am. J. Physiol Regul. Integr. Comp. Physiol.* **293**, R1545-R1551.

Fernando, P. and Megeney, L. A. (2007). Is caspase-dependent apoptosis only cell differentiation taken to the extreme? *FASEB J.* **21**, 8-17.

Frame, S. and Cohen, P. (2001). GSK3 takes centre stage more than 20 years after its discovery. *Biochem. J.* **359**, 1-16.

Goodell, M. A., Jackson, K. A., Majka, S. M., Mi, T., Wang, H., Pocius, J., Hartley, C. J., Majesky, M. W., Entman, M. L., Michael, L. H. et al. (2001). Stem cell plasticity in muscle and bone marrow. *Ann. N. Y. Acad. Sci.* **938**, 208-218.

Gussoni, E., Blau, H. M. and Kunkel, L. M. (1997). The fate of individual myoblasts after transplantation into muscles of DMD patients. *Nat. Med.* **3**, 970-977.

Hollnagel, A., Grund, C., Franke, W. W. and Arnold, H. H. (2002). The cell adhesion molecule M-cadherin is not essential for muscle development and regeneration. *Mol. Cell Biol.* **22**, 4760-4770.

Hongisto, V., Smeds, N., Brecht, S., Herdegen, T., Courtney, M. J. and Coffey, E. T. (2003). Lithium blocks the c-Jun stress response and protects neurons via its action on glycogen synthase kinase 3. *Mol. Cell Biol.* **23**, 6027-6036.

Irintchev, A., Zeschnigk, M., Starzinski-Powitz, A. and Wernig, A. (1994). Expression pattern of M-cadherin in normal, denervated, and regenerating mouse muscles. *Dev. Dyn.* **199**, 326-337.

Jahnke, V. E., Sabido, O. and Freyssenet, D. (2009). Control of mitochondrial biogenesis, ROS level, and cytosolic Ca2+ concentration during the cell cycle and the onset of differentiation in L6E9 myoblasts. *Am. J. Physiol Cell Physiol.* **296**, C1185-C1194.

Jejurikar, S. S. and Kuzon, W. M., Jr (2003). Satellite cell depletion in degenerative skeletal muscle. *Apoptosis.* **8**, 573-578.

Jejurikar, S. S., Henkelman, E. A., Cederna, P. S., Marcelo, C. L., Urbanchek, M. G. and Kuzon, W. M., Jr (2006). Aging increases the susceptibility of skeletal muscle derived satellite cells to apoptosis. *Exp. Gerontol.* **41**, 828-836.

Kaga, S., Zhan, L., Altaf, E. and Maulik, N. (2006). Glycogen synthase kinase-3beta/beta-catenin promotes angiogenic and anti-apoptotic signaling through the induction of VEGF, Bcl-2 and survivin expression in rat ischemic preconditioned myocardium. *J. Mol. Cell Cardiol.* **40**, 138-147.

Kaupmann, K., Becker-Follmann, J., Scherer, G., Jockusch, H. and Starzinski-Powitz, A. (1992). The gene for the cell adhesion molecule M-cadherin maps to mouse chromosome 8 and human chromosome 16q24.1-qter and is near the E-cadherin (uvomorulin) locus in both species. *Genomics* **14**, 488-490.

Kinnard, R. S., Mylabathula, D. B., Uddemarri, S., Rice, K. M., Wright, G. L. and Blough, E. R. (2005). Regulation of p70S6k, GSK-3beta, and calcineurin in rat striated muscle during aging. *Biogerontology.* **6**, 173-184.

Koutsouki, E., Beeching, C. A., Slater, S. C., Blaschuk, O. W., Sala-Newby, G. B. and George, S. J. (2005). N-cadherin-dependent cell-cell contacts promote human saphenous vein smooth muscle cell survival. *Arterioscler. Thromb. Vasc. Biol.* **25**, 982-988.

Leiter, J. R. and Anderson, J. E. (2010). Satellite cells are increasingly refractory to activation by nitric oxide and stretch in aged mouse-muscle cultures. *Int. J. Biochem. Cell Biol.* **42**, 132-136.

Linseman, D. A., Butts, B. D., Precht, T. A., Phelps, R. A., Le, S. S., Laessig, T. A., Bouchard, R. J., Florez-McClure, M. L. and Heidenreich, K. A. (2004). Glycogen synthase kinase-3beta phosphorylates Bax and promotes its mitochondrial localization during neuronal apoptosis. *J. Neurosci.* **24**, 9993-10002.

Lippens, S., Denecker, G., Ovaere, P., Vandenabeele, P. and Declercq, W. (2005). Death penalty for keratinocytes: apoptosis versus cornification. *Cell Death. Differ.* **12** Suppl 2, 1497-1508.

Ma, C., Bower, K. A., Chen, G., Shi, X., Ke, Z. J. and Luo, J. (2008). Interaction between ERK and GSK3beta mediates basic fibroblast growth factor-induced apoptosis in SK-N-MC neuroblastoma cells. *J. Biol. Chem.* **283**, 9248-9256.

Maurer, U., Charvet, C., Wagman, A. S., Dejardin, E. and Green, D. R. (2006). Glycogen synthase kinase-3 regulates mitochondrial outer membrane permeabilization and apoptosis by destabilization of MCL-1. *Mol. Cell* **21**, 749-760.

Ott, M., Zhivotovsky, B. and Orrenius, S. (2007). Role of cardiolipin in cytochrome c release from mitochondria. *Cell Death. Differ.* **14**, 1243-1247.

Partridge, T., Lu, Q. L., Morris, G. and Hoffman, E. (1998). Is myoblast transplantation effective? *Nat. Med.* **4**, 1208-1209.

Patel, S., Doble, B. W., MacAulay, K., Sinclair, E. M., Drucker, D. J. and Woodgett, J. R. (2008). Tissue-specific role of glycogen synthase kinase 3beta in glucose homeostasis and insulin action. *Mol. Cell Biol.* **28**, 6314-6328.

Pearce, N. J., Arch, J. R., Clapham, J. C., Coghlan, M. P., Corcoran, S. L., Lister, C. A., Llano, A., Moore, G. B., Murphy, G. J., Smith, S. A. et al. (2004). Development of glucose intolerance in male transgenic mice overexpressing human glycogen synthase kinase-3beta on a muscle-specific promoter. *Metabolism* **53**, 1322-1330.

Quadrilatero, J. and Bloemberg, D. (2010). Apoptosis repressor with caspase recruitment domain is dramatically reduced in cardiac, skeletal, and vascular smooth muscle during hypertension. *Biochem. Biophys. Res. Commun.* **391**, 1437-1442.

Quadrilatero, J. and Rush, J. W. (2008). Evidence for a pro-apoptotic phenotype in skeletal muscle of hypertensive rats. *Biochem. Biophys. Res. Commun.* **368**, 168-174.

Rochard, P., Cassar-Malek, I., Marchal, S., Wrutniak, C. and Cabello, G. (1996). Changes in mitochondrial activity during avian myoblast differentiation: influence of triiodothyronine or v-erb A expression. *J. Cell Physiol.* **168**, 239-247.

Rochard, P., Rodier, A., Casas, F., Cassar-Malek, I., Marchal-Victorion, S., Daury, L., Wrutniak, C. and Cabello, G. (2000). Mitochondrial activity is involved in the regulation of myoblast differentiation through myogenin expression and activity of myogenic factors. *J. Biol. Chem.* **275**, 2733-2744.

Sajko, S., Kubinova, L., Cvetko, E., Kreft, M., Wernig, A. and Erzen, I. (2004). Frequency of M-cadherin-stained satellite cells declines in human muscles during aging. *J. Histochem. Cytochem.* **52**, 179-185.

Seale, P. and Rudnicki, M. A. (2000). A new look at the origin, function, and "stem-cell" status of muscle satellite cells. *Dev. Biol.* **218**, 115-124.

Shiina, K., Gohda, T., Murakoshi, M., Yamada, K., Aoki, T., Yamazaki, T., Tanimoto, M. and Tomino, Y. (2007). M-cadherin, a candidate gene for type 2 diabetes and related phenotypes in a KK/Ta mouse model. *Acta. Diabetol.* **44**, 6-13.

Siu, P. M. and Alway, S. E. (2005). Mitochondria-associated apoptotic signalling in denervated rat skeletal muscle. *J. Physiol.* **565**, 309-323.

Siu, P. M., Pistilli, E. E. and Alway, S. E. (2005a). Apoptotic responses to hindlimb suspension in gastrocnemius muscles from young adult and aged rats. *Am. J. Physiol Regul. Integr. Comp. Physiol.* **289**, R1015-R1026.

Siu, P. M., Pistilli, E. E., Butler, D. C. and Alway, S. E. (2005b). Aging influences cellular and molecular responses of apoptosis to skeletal muscle unloading. *Am. J. Physiol. Cell Physiol.* **288**, C338-C349.

Siu, P. M., Pistilli, E. E., Ryan, M. J. and Alway, S. E. (2005c). Aging sustains the hypertrophy-associated elevation of apoptotic suppressor X-linked inhibitor of apoptosis protein (XIAP) in skeletal muscle during unloading. *J. Gerontol. A. Biol. Sci. Med. Sci.* **60**, 976-983.

Siu, P. M., Wang, Y. and Alway, S. E. (2009). Apoptotic signaling induced by H2O2-mediated oxidative stress in differentiated C2C12 myotubes. *Life Sci.* **84**, 468-481.

Tews, D. S. and Goebel, H. H. (1997). DNA-fragmentation and expression of apoptosis-related proteins in muscular dystrophies. *Neuropathol. Appl. Neurobiol.* **23**, 331-338.

Tidball, J. G., Albrecht, D. E., Lokensgard, B. E. and Spencer, M. J. (1995). Apoptosis precedes necrosis of dystrophin-deficient muscle. *J. Cell Sci.* **108 (Pt 6)**, 2197-2204.

van den Eijnde, S. M., van den Hoff, M. J., Reutelingsperger, C. P., van Heerde, W. L., Henfling, M. E., Vermeij-Keers, C., Schutte, B., Borgers, M. and Ramaekers, F. C. (2001). Transient expression of phosphatidylserine at cell-cell contact areas is required for myotube formation. *J. Cell Sci.* **114**, 3631-3642.

van der Velden, J. L., Langen, R. C., Kelders, M. C., Wouters, E. F., Janssen-Heininger, Y. M. and Schols, A. M. (2006). Inhibition of glycogen synthase kinase-3beta activity is sufficient to stimulate myogenic differentiation. *Am. J. Physiol. Cell Physiol.* **290**, C453-C462.

van der Velden, J. L., Langen, R. C., Kelders, M. C., Willems, J., Wouters, E. F., Janssen-Heininger, Y. M. and Schols, A. M. (2007). Myogenic differentiation during regrowth of atrophied skeletal muscle is associated with inactivation of GSK-3beta. *Am. J. Physiol Cell Physiol.* **292**, C1636-C1644.

Vyas, D. R., Spangenburg, E. E., Abraha, T. W., Childs, T. E. and Booth, F. W. (2002). GSK-3beta negatively regulates skeletal myotube hypertrophy. *Am. J. Physiol Cell Physiol.* **283**, C545-C551.

Walsh, K. (1997). Coordinate regulation of cell cycle and apoptosis during myogenesis. *Prog. Cell Cycle Res.* **3**, 53-58.

Watcharasit, P., Bijur, G. N., Song, L., Zhu, J., Chen, X. and Jope, R. S. (2003). Glycogen synthase kinase-3beta (GSK3beta) binds to and promotes the actions of p53. *J. Biol. Chem.* **278**, 48872-48879.

Williamson, C. L., Dabkowski, E. R., Baseler, W. A., Croston, T. L., Alway, S. E. and Hollander, J. M. (2010). Enhanced apoptotic propensity in diabetic cardiac mitochondria: influence of subcellular spatial location. *Am. J. Physiol. Heart Circ. Physiol.* **298**, H633-H642.

Wrobel, E., Brzoska, E. and Moraczewski, J. (2007). M-cadherin and beta-catenin participate in differentiation of rat satellite cells. *Eur. J. Cell Biol.* **86**, 99-109.

Zammit, P. S., Partridge, T. A. and Yablonka-Reuveni, Z. (2006). The skeletal muscle satellite cell: the stem cell that came in from the cold. *J. Histochem. Cytochem.* **54**, 1177-1191.

Journal of Cell Science